

# The Application Adaptability of Gimbal Structure in the Joint Connection of Daily Life Products

Tianhang Ma \*

Beijing Chaoyang Tongwen Foreign Language School, Beijing, 100015, China

\* Corresponding Author Email: zhouzhuge78@gmail.com

**Abstract.** This study investigates the structural adaptability and optimization of gimbal mechanisms in the joint connections of daily-use products. Traditional joint structures, such as hinges and rotary shafts, often exhibit limited flexibility, instability, and gradual loosening, compromising safety and comfort over the long term. To address these issues, a novel gimbal-based joint design is proposed, emphasizing multi-degree-of-freedom movement and passive stabilization without complex control systems. Through torsional dynamic modeling and parametric simulations, the relationships between stiffness, damping, and external disturbances are quantitatively analyzed. Simulation results reveal that the optimal performance balance is achieved within a medium stiffness (0.2–0.4 N·m/rad) and damping range (0.08–0.15 N·m·s/rad), ensuring fast stabilization and strong resistance to oscillation. Compared to conventional joints, the gimbal structure offers enhanced anti-disturbance performance, smoother adjustment, and better adaptability to external forces. This research provides theoretical and practical guidance for integrating gimbal mechanisms into household applications, including lamps, brackets, and folding furniture. Future work will focus on multi-axis coupling modeling, experimental validation, and fatigue testing to verify the long-term reliability of the design and promote the lightweight, modular evolution of gimbal-based mechanisms in daily products.

**Keywords:** Gimbal mechanism, Joint connection design, Dynamic modeling, Parametric simulation.

## 1. Introduction

With the development of the social economy and the improvement of living standards, consumers' demands for daily necessities are shifting from single-function satisfaction to high-quality experiences, multi-functional integration, and longer lifespans. Joint connections, as crucial components of furniture, kitchenware, and small household appliances, directly affect the stability, flexibility, and durability of these products. However, traditional structures such as hinges and rotating shafts have obvious shortcomings: furniture joints tend to loosen over time, affecting storage safety; the joint adjustment range of kitchenware is limited, making it challenging to meet diverse operating requirements. Usually, small household devices do not stay in place when subjected to minor jolting forces and thus lack stability. These problems limit product efficiency and complicate users' reference experience, serving as a primary barrier to design ascendancy.

To overcome the impasse, it is first necessary to address the internal structural design. The pan-tilt model can support and control multiple attitudes by adjusting degrees of freedom [1-5]. It is worth noting that, in recent years, this principle has been successfully incorporated into sectors such as navigation, aviation, aerospace, and robotics [6]. Its benefit lies in obtaining angle change via the collective operation of multi-axis and in its compensation mechanism for external disturbances, which serves as convenient dampers or added weights, stabilizing the attitude [7]. Accompanying this trend is the growing popularity of joints for daily objects. On the one hand, multi-angle stepless adjustment, which can be achieved without force, increases operability. On the other hand, it reduces disturbance and solves the problems of loosening and displacement common to traditional designs [8].

The significance of the pan-tilt structure is reflected at both the user and industry levels. For users, it can significantly enhance the experience, such as multi-angle adjustable table and chair brackets, anti-shake and stable water cups, and lighting equipment, improving comfort and safety. For the industry, it provides new ideas for joint design innovation, promotes the upgrade of daily necessities from traditional machinery to intelligent systems, and helps products compete more effectively.

Compared with conventional structures, pan-tilt units offer clear advantages in terms of freedom, anti-disturbance performance, and scalability, creating conditions for entering the civilian market.

Based on this, this study focuses on the adaptability of the pan-tilt structure in the joint connection of daily necessities. It explores its feasibility and value in different application scenarios. The research follows the logic of "raising questions, understanding the latest research progress, establishing dynamic models, parametric simulation, and compatibility analysis": Firstly, analyze the convergence point between the characteristics of the pan-tilt and the demands of daily necessities; Secondly, establish an evaluation framework from three dimensions: structure, performance and cost; Finally, combined with the simulation code data, analyze the degree to which the pan-tilt structure affects the peak Angle, summarize its application potential and limitations, and look forward to the future development direction.

From an academic perspective, this study aims to "migrate" the pan-tilt structure from the industrial field into civilian daily use, thereby representing a cross-border innovation in structural principles. It not only enriches the theoretical system of mechanical structure design, but also provides a new passive stability and multi-angle adjustment solution for daily necessities. From an application perspective, with the popularization of smart homes and portable devices, users' demand for features such as "adjustable", "anti-shake", and "low noise" is increasing daily. If the pan-tilt structure can achieve these characteristics at a low cost and purely mechanically, it will have significant market competitiveness.

Based on this, the following objectives are set for this study. Theoretical objective: To construct a simplified dynamic model of the pan-tilt structure in daily necessities and analyze the coupling relationship among stiffness, damping, and disturbing forces. Simulation Objective: Through parametric simulation, study the influence of different structural parameters on the performance against disturbances, and determine the optimal parameter range suitable for civilian scenarios. Design Objective: Establish a comprehensive evaluation framework covering structural performance, cost, and adaptability, and propose feasible product design cases. Ultimately, this study aims to provide a method for achieving "passive intelligence" at the structural level for daily necessities, enabling them to deliver stable, flexible, and durable performance without the need for complex electronic systems.

## 2. Research Methods

This research takes "dynamic modeling combined with parametric simulation" as its core research path, aiming to explore the performance boundaries and design rules of pan-head joints in daily necessities through quantitative model analysis and numerical simulation.

### 2.1. Simplify the establishment of the dynamic model

In a complex pan-tilt structure, the coupling, support methods, and damping distribution between the axes can be highly complex. To extract the main influencing factors, this study simplifies them into a non-standard second-order rotational system, the rotational vibration equation (e.g., the dynamic equation of a single-degree-of-freedom rotational system) [1].

$$J\theta'' + c\theta' + k\theta = T(t) \quad (1)$$

Among them:

J: The moment of inertia of the system, with a value of 0.01 kg·m<sup>2</sup> (this value refers to the typical inertia range of lightweight mechanical systems such as small brackets and rotating parts of household appliances);

c: Damping coefficient, reflecting the energy dissipation capacity;

k: Stiffness coefficient, which reflects the structure's resistance to deformation;

T (t): External disturbance torque, simulated in pulse form for short-term impact or shaking in daily use (amplitude 0.2 N·m, duration 0.02 s).

This model can effectively capture the pan-tilt's dynamic response to minor disturbances [1]. By changing the damping and stiffness parameters, the attitude stability and response speed of the structure under different working conditions can be analyzed, thereby providing a theoretical basis for subsequent optimization.

## 2.2. Parametric Simulation Design

To comprehensively evaluate the dynamic performance of the pan-tilt structure, this study conducts a parametric analysis using the Python simulation platform [9]. The specific process is as follows:

### 2.2.1. Parameter range setting

Combining the typical force characteristics of furniture, kitchenware, and small household appliances, the stiffness ( $k$ ) is set at 0.01-2.0 N·m/rad, and the damping ( $c$ ) is set at 0.001-1.0 N·m·s/rad. Low stiffness (0.01-0.1) corresponds to flexible joints, such as cups and brackets. Medium stiffness (0.3-1.0) is suitable for adjustable lamps or display brackets. High rigidity ( $>1.0$ ) is ideal for load-bearing structures, such as folding tables and chairs.

### 2.2.2. Definition of Performance Indicators

To quantify the structure's stability and responsiveness, the following three indicators are selected. The Peak Angle reflects the structure's resistance to instantaneous disturbances. Time to stabilization have showed the efficiency with which the system returns to stability. Root means square Angle is used to measure the degree of attitude fluctuation under long-term use.

### 2.2.3. Simulation and Visualization Process

Figure 1 establishes a second-order rotating system based on the dynamic equation of a single-degree-of-freedom rotating system, defines inertia, damping, stiffness, and disturbance moment, sets stiffness ( $k=0.01-2.0$ ) N·m/rad and damping ( $c=0.001- 1.0$ ) N·m·s/rad, and generates parameter combinations.

Figure 2 shows the integration of the equation to obtain the angle-time response curve. Figure 3 calculates the peak Angle, stabilization time, and root-mean-square Angle, and interpolates and corrects outliers. Figures 4, 5, and 6 show the response curves and heat maps generated with Matplotlib to demonstrate performance differences across different parameters visually.

```
>>> import numpy as np
... import matplotlib.pyplot as plt
... from scipy.integrate import solve_ivp
... from scipy import signal
...
... # -----
... # 1. system parameter
... # -----
... J = 0.01 # rotational inertia
... T_amp = 0.2 # external disturbance torque amplitude
... T_duration = 0.02 # duration of disturbance (s)
...
... # external disturbance torque function
... def torque(t):
...     return T_amp if t < T_duration else 0.0
... # kinetic equation
... def model(t, y, c, k):
...     theta, omega = y
...     dydt = [omega, (torque(t) - c * omega - k * theta) / J]
...     return dydt
...
... # time horizon
... t_span = [0, 3]
... t_eval = np.linspace(0, 3, 1000)
```

Figure 1. System parameter

```

... # -----
... # 2. single set of parameters: angle-time response curve
... # -----
... c0, k0 = 0.1, 0.3
... sol = solve_ivp(model, t_span, [0, 0], args=(c0, k0), t_eval=t_eval)
... theta = sol.y[0]
...
... plt.figure(figsize=(7,4))
... plt.plot(sol.t, theta*180/np.pi, label=f'c={c0}, k={k0}')
... plt.xlabel('time t (s)')
... plt.ylabel('angle $\theta$  (°)')
... plt.title('angle-time response curve')
... plt.grid(True)
... plt.legend()
... plt.tight_layout()
... plt.show()
...

```

**Figure 2.** Single set of parameters

```

>>> # -----
... # 3. comparison of multi-parameter response curves
... # -----
... plt.figure(figsize=(7,4))
... for c in [0.05, 0.1, 0.2, 0.5]:
...     sol = solve_ivp(model, t_span, [0, 0], args=(c, 0.3), t_eval=t_eval)
...     plt.plot(sol.t, sol.y[0]*180/np.pi, label=f'c={c}')
...
... plt.xlabel('time t (s)')
... plt.ylabel('angle  $\theta$  (°)')
... plt.title('comparison of response curves under different damping coefficient\
ts')
... plt.legend()
... plt.grid(True)
... plt.tight_layout()
... plt.show()
...

```

**Figure 3.** Comparison of multi-parameter response curves

```

>>> # -----
... # 4. peak angle heat map
... # -----
... k_values = np.linspace(0.01, 2.0, 40)
... c_values = np.linspace(0.001, 1.0, 40)
... peak_angle = np.zeros((len(k_values), len(c_values)))
...
... for i, k in enumerate(k_values):
...     for j, c in enumerate(c_values):
...         sol = solve_ivp(model, [0, 2], [0, 0], args=(c, k), t_eval=np.linspace(0,2,500))
...         peak_angle[i, j] = np.max(np.abs(sol.y[0])) * 180/np.pi
...
... plt.figure(figsize=(7,5))
... plt.imshow(peak_angle, extent=[c_values[0], c_values[-1], k_values[0], k_values[-1]],
...             origin='lower', aspect='auto', cmap='plasma')
... plt.colorbar(label='peak angle (°)')
... plt.xlabel('damping coefficient c (N·m·s/rad)')
... plt.ylabel('stiffness k (N·m/rad)')
... plt.title('peak angle distribution heat map')
... plt.tight_layout()
... plt.show()
...

```

**Figure 4.** Peak angle heat map

```

>>> # -----
... # 5. Bode amplitude frequency diagram
... # -----
... # transfer function:  $\theta(s)/T(s) = 1 / (J*s^2 + c*s + k)$ 
... c_test, k_test = 0.1, 0.3
... num = [1]
... den = [J, c_test, k_test]
... sys = signal.lti(num, den)
... w, mag, phase = signal.bode(sys)
...
... plt.figure(figsize=(7,4))
... plt.semilogx(w, mag)
... plt.title('Bode amplitude-frequency response graph')
... plt.xlabel('angular frequency  $\omega$  (rad/s)')
... plt.ylabel('amplitude (dB)')
... plt.grid(True, which='both', ls='--')
... plt.tight_layout()
... plt.show()

```

Figure 5. Bode amplitude frequency diagram

```

>>> # -----
... # 6. time-domain response curve(step input)
... # -----
... t_step, y_step = signal.step(sys)
... plt.figure(figsize=(7,4))
... plt.plot(t_step, y_step)
... plt.title('time-domain step response curve')
... plt.xlabel('time t (s)')
... plt.ylabel('angle  $\theta$  (rad)')
... plt.grid(True)
... plt.tight_layout()
... plt.show()

```

Figure 6. Time-domain response curve

#### 2.2.4. Correction

Make numerical corrections to the outliers in the simulation results. The criterion for determining outliers is that the peak Angle exceeds  $10^\circ$  (since the maximum acceptable peak Angle for daily necessities such as water cups is  $5^\circ$ , exceeding  $10^\circ$  falls outside the practical application range). The correction method uses interpolation replacement: abnormal data are replaced by the average of the combination results of adjacent normal parameters. At the same time, eliminate parameter combinations that exceed the actual manufacturing capacity to ensure the subsequent design is engineering-feasible.

### 3. Analysis of the adaptability of the pan-tilt structure

By analyzing simulation results for different combinations of stiffness and damping parameters, the performance laws and fit boundaries of cloud platform structures for daily use can be summarized [8,9].

Figure 1 shows the change in the system's Angle under a single disturbance, and Figure 2 shows the Dynamic responses under different damping coefficients. Figure 3 shows the influence of stiffness-damping parameters on performance. Figure 4 presents the frequency-domain characteristics of the system. Figure 5 demonstrates the system's stability and recovery speed.

Under the action of a typical pulse disturbance torque (amplitude  $0.2 \text{ N}\cdot\text{m}$ , duration  $0.02 \text{ s}$ ), the angle-time response curve of the system is shown in Figure 1. The results show that the pan-tilt structure exhibits typical second-order underdamped behavior over the parameter range  $k = 0.1\text{-}0.5 \text{ N}\cdot\text{m}/\text{rad}$  and  $c = 0.05\text{-}0.2 \text{ N}\cdot\text{m}\cdot\text{s}/\text{rad}$ . When the damping coefficient is relatively small ( $c < 0.08$ ), the system exhibits apparent oscillation; the peak Angle can reach  $7^\circ$ , the stabilization time exceeds 2

seconds, and the stability is insufficient. As the damping increases ( $c=0.1-0.2$ ), the system response smooths significantly, the peak Angle drops to  $2^{\circ}-4^{\circ}$ , and the stabilization time shortens to 1-1.5 seconds. The influence trend of stiffness is similar to that of damping: low-stiffness structures ( $k<0.1$ ) are excessively flexible and prone to disturbances. Although the high-stiffness structure ( $k > 0.5$ ) is stable, the adjustment feel is stiff, and the user experience suffers. A comprehensive comparison shows that the parameter combinations near ( $k=0.3$ ) and ( $c=0.1$ ) can achieve the optimal response balance.

The comparison of multiple sets of response curves (Figure 2) shows a significant coupling between the effects of stiffness and damping on system performance. When stiffness is low, the system is susceptible to changes in damping, and even slight damping can lead to increased overshoot. As stiffness increases, the system's anti-disturbance performance improves, but if damping is too high, it can cause response lag. In the medium stiffness and medium damping range ( $(k\approx 0.3, c\approx 0.1)$ ), the system can respond quickly and effectively suppress oscillation, which is the optimal design range. This result indicates that, in actual design, the principle of "stiffness-damping coordinated parameter adjustment" should be adopted rather than strengthening a single parameter. For daily necessities, this medium-damping state can achieve a good balance between smooth touch and structural stability.

As shown in Figures 3,7-11, through simulation calculations of different combinations of ( $k$ ) and ( $c$ ) parameters, a distribution heat map of the peak Angle and the time to stabilization was drawn. The results show that a distinct performance gradient distribution is observed in the parameter space: the color in the lower-left region (low ( $k$ ), low ( $c$ )) is the brightest, corresponding to a large peak Angle and an apparent system oscillation. The upper-right area (high ( $k$ ), high ( $c$ )) is darker, and the system responds smoothly but lacks flexibility. The middle region ( $(k=0.25-0.4, c=0.08-0.15)$ ) forms the optimal performance zone. The peak Angle of the system in this area is usually less than  $5^{\circ}$ , and the stabilization time is approximately 1 second, taking both stability and response speed into account. The heat map results are consistent with the theoretical model analysis, further verifying the accuracy and guiding value of parametric simulation.

The frequency-domain characteristics of the system are shown in Figure 4. According to the Bode amplitude-frequency curve, within the range of ( $k=0.1-0.5$ ) and ( $c=0.05-0.2$ ), the natural frequency of the system ( $\omega = \sqrt{k/J}$ ) is approximately 3-7 rad/s, corresponding to the actual frequency of 0.5-1 Hz [5,6]. This frequency range is close to the frequencies of human operation and desktop vibration, and thus is a key section that affects the anti-interference performance of daily necessities. When the damping is small ( $c<0.1$ ), the system shows a slight formant at the natural frequency. As damping increases, the amplitude-frequency curve transitions smoothly, indicating that damping significantly inhibits resonance amplification. Overall, the pan-tilt structure has excellent low-pass characteristics in the mid-frequency band and can effectively filter out external high-frequency disturbances, thereby achieving passive stabilization.

The time-domain response curve under the step moment input is shown in Figure 5. The results show that the steady-state Angle of the system is inversely proportional to the stiffness, while damping mainly affects response speed and overshoot. When ( $k=0.3, c=0.1$ ), the steady-state Angle of the system is approximately 0.7 rad ( $\approx 40^{\circ}$ ), the rise time is 1.2 s, and there is no apparent oscillation [2,10]. When the damping is small ( $c=0.05$ ), an overshoot of approximately 15% occurs, while when the damping is too large ( $c=0.2$ ), the rise time increases by about 40%. Therefore, under the premise of meeting steady-state accuracy, medium damping should be given priority to achieve a fast, smooth response. This rule provides a quantifiable basis for the "smooth adjustment" and "buffering and anti-shake" functions of the joints of daily necessities.

Based on the results of both time-domain and frequency-domain analyses, the following conclusions can be drawn. Stiffness mainly determines anti-interference capability, while damping mainly determines system stability and response speed. The medium parameter range ( $k=0.2-0.4, c=0.08-0.15$ ) offers optimal performance, balancing shock resistance, flexibility, and smoothness. The system's natural frequency is close to the human body's operating frequency. Attention should be paid to avoiding resonance superposition in product design. 4. Parametric simulation can predict

the experience trend, providing a quantitative basis for the optimization of the pan-tilt structure in the joint design of daily necessities.

Overall, the simulation results of this study show that the pan-tilt structure can significantly enhance the anti-disturbance and stability of the joints of daily necessities under appropriate parameter configurations, achieving a "passive intelligent" adjustment function at the structural level and providing reliable theoretical support for subsequent prototype design and actual manufacturing.

The results show that under conditions of low damping ( $c < 0.03$ ) and low stiffness ( $k < 0.1$ ), the structure exhibits pronounced excessive flexibility [7,9,11], with excessive peak angles and poor stability. However, under conditions of high stiffness ( $k > 1.0$ ) or high damping ( $c > 0.5$ ), although stability is enhanced, the adjustment response slows, the hand feel becomes stiff, and this is not conducive to the flexibility of daily use. The optimal performance balance range is concentrated in:  $k = 0.1-0.5 \text{ N}\cdot\text{m}/\text{rad}$ ,  $c = 0.05-0.2 \text{ N}\cdot\text{m}\cdot\text{s}/\text{rad}$ . Within this range, the system's peak Angle can generally be controlled to within  $5^\circ$ , and the stabilization time is between 1 and 1.5 seconds.

Based on the clustering analysis of performance indicators, the parameter intervals are divided into three application areas: 1. Flexible anti-shake type (Class F): Low stiffness and low damping, suitable for lightweight items such as water cups and portable stands; 2. Balanced steady-state type (Class B): Medium stiffness and medium damping, ideal for products such as lighting fixtures and display supports that require flexible adjustment; 3. Rigid support type (R class): High rigidity and medium damping, suitable for load-bearing furniture structures [12-14].

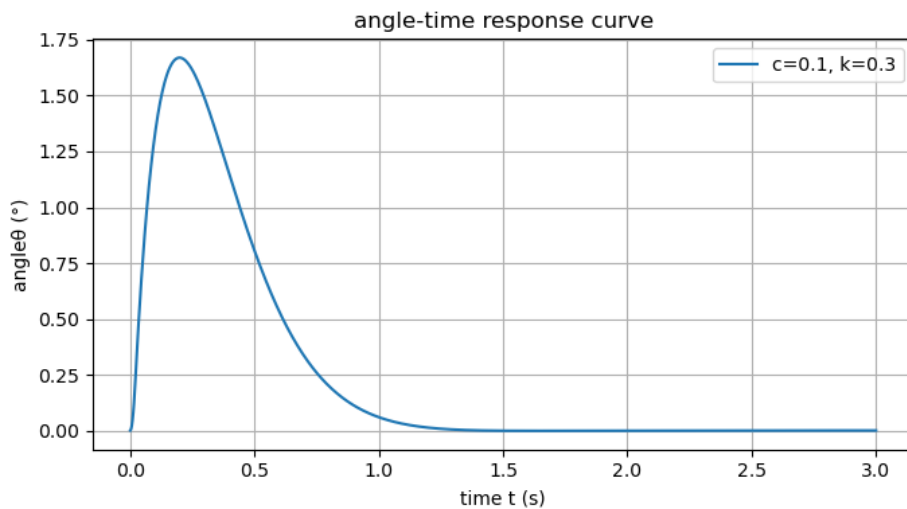


**Figure 7.** Angle-time response curve

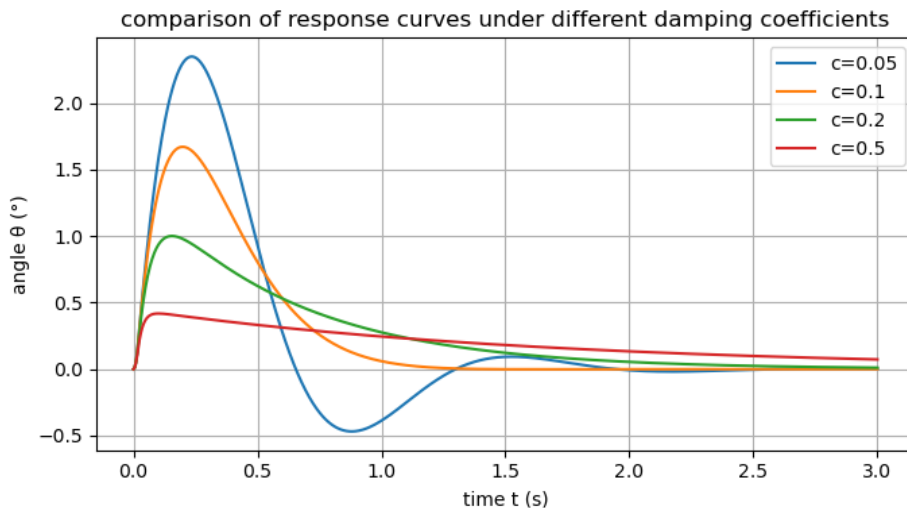


**Figure 8.** Comparison of response curves under different damping coefficients

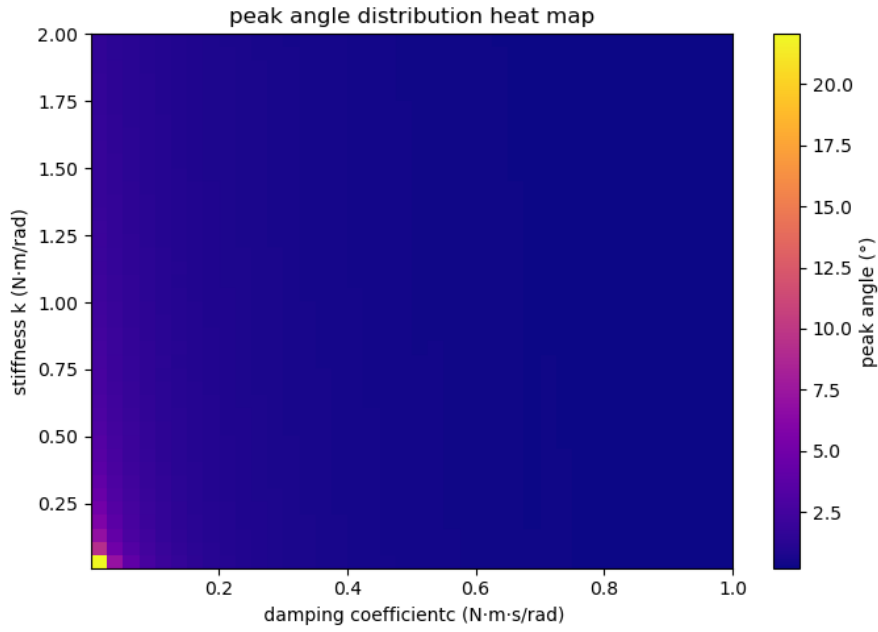


**Figure 9.** Peak angle distribution heat map

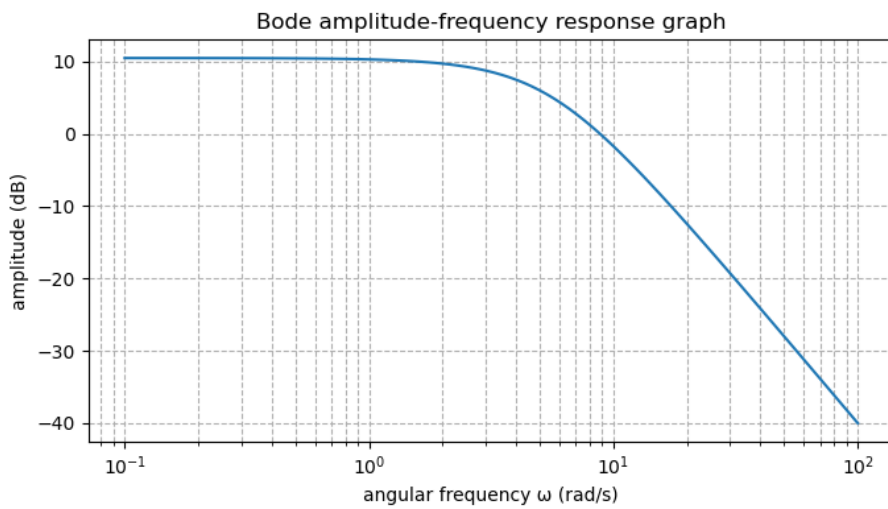


**Figure 10.** Bode amplitude-frequency response graph

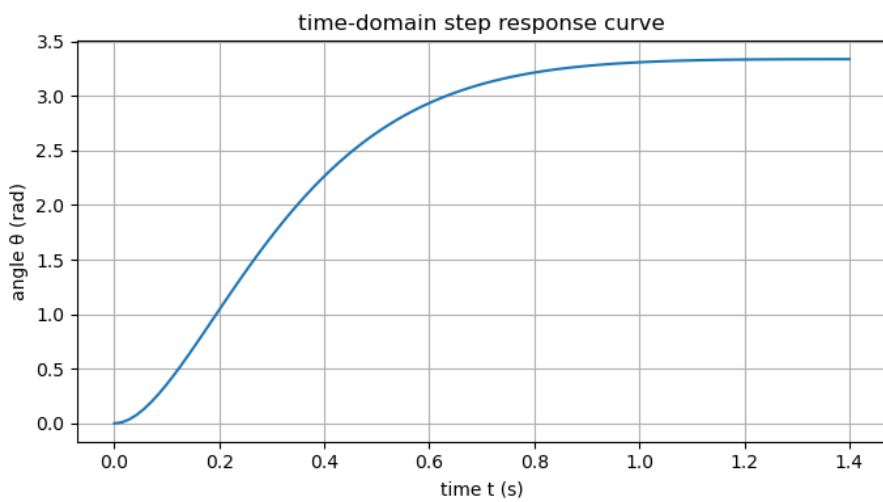


**Figure 11.** Time-domain step response curve

## 4. Conclusion

This study takes the adaptability of the pan-tilt structure in daily use as the core issue. It proposes a new approach to introducing multi-degree-of-freedom support mechanisms into civilian products. Dynamics modeling based on combined Python numerical simulation and performance distribution analysis uncovers the coupling rule of damping, stiffness, and disturbing forces. The conclusion is that reasonable parameter matching enables the joint connections to achieve strong stability and smoothness, and in its passive state, the structure possesses self-stabilizing properties. These findings open the door to designing lightweight, multi-angle, and sustainable goods.

Theoretically, this paper integrates the mechanical vibration principle into the optimization of flexible structures and demonstrates the practicality of the pan-tilt principle in miniature structures. In terms of application, its research findings can be widely applied to lamps, shelf supports, tables, chairs, and so on, to solve the anti-disturbing problem for end users' products at a low cost. At the same time, two aspects of follow-up development work were proposed: the first is to perform multi-axis coupling modeling to improve simulation precision; the second is to validate actual performance through experimental tests combined with optimized materials. As a whole, this study not only facilitates structural innovation but also demonstrates an alternative engineering route for the design upgrade of innovative living products.

While this article confirms the feasibility of using pan-tilt structures for daily tasks through dynamic modeling and parametric simulation, several challenges remain to be addressed.

**Restriction to Single-Axis Torsion:** The current model assumes a simplified single-axis torsion model. The coupling effect between multiple rotation axes and the nonlinear damping during large-amplitude motion have not been fully considered. A more advanced full-range, multi-degree-of-freedom coupling model will be necessary to fine-tune and predict the device's in vivo performance.

Second, the results obtained here are entirely based on numerical methods, and experimental validation, including prototype fabrication and vibration testing, is desired to verify theoretical predictions and evaluate the feasibility for manufacturing under material and cost constraints.

Lastly, the role of long-term performance factors, i.e., wear, fatigue, and environmental effects, was outside the scope of this study. These effects should be considered in the long-term durability design and life cycle cost optimization, which will be part of our future work. Lastly, the use of lightweight materials and modular concepts can lead to even greater adaptability of the pan-tilt mechanism in consumer applications. Investigation along those lines will enable the theory to apply to practical engineering problems and facilitate the development of intelligent, stable, and easy-to-use designs in daily products.

## References

- [1] Rao S. *Mechanical Vibrations* (6th ed.). Pearson Education, 2011.
- [2] Chen Z, Chen G, Zhang X. Damped leaf flexure hinge: theoretical model and experiments—Review of Scientific Instruments, 2015, 86 (5): 055002.
- [3] Chen Y, Zhang X, Zhao H. Design and control of gimbal systems for stabilization applications. *IEEE/ASME Transactions on Mechatronics*, 2018, 23 (4): 1675 – 1685.
- [4] Huang Q, et al. Modeling and control of a two-axis stabilized gimbal via the Kane method. *Sensors*, 2024, 24 (11): 3615.
- [5] Wang C, Zhang P, Li T, et al. Robust control for a dual-axis stabilized platform using an adaptive sliding mode algorithm. *IEEE Access*, 2022, 10: 75112 – 75123.
- [6] Altan A, et al. Model predictive control of three-axis gimbal system. *ISA Transactions*, 2020, 100: 235 – 246.
- [7] Lin J, et al. Design and analysis of a triangular bi-axial flexure hinge. *Proceedings of the Institution of Mechanical Engineers, Part C: Journal of Mechanical Engineering Science*, 2023, 237 (2): 988 – 999.

- [8] Cammarata A, Maddio P D, et al. Dynamic model of a conjugate surface flexure hinge. *Micromachines*, 2022, 13 (6): 957.
- [9] Chang Y S, et al. Optimal design of a leaf flexure compliant mechanism with damping layers. *Micromachines*, 2022, 13 (6): 817.
- [10] Chen Z, et al. Damped circular hinge with integrated comb-like substructures. *Mechanism and Machine Theory*, 2018, 122: 68 – 85.
- [11] Liu M, et al. multi-material topology optimization of flexure hinges. *Micromachines*, 2022, 13: 1414.
- [12] Agasti A, Hazarika A, Bhikkaji B. Adaptive backstepping control for line-of-sight stabilization in electro-optical tracking platforms. *Mechanical Systems and Signal Processing*, 2023, 198: 110454.
- [13] Kouhi H, Kabganian M, et al. Dynamic modeling and vibration suppression of gimballed thrusters for spacecraft attitude control. *Acta Astronautica*, 2024, 215: 32 – 45.
- [14] Virtanen P, et al. SciPy 1.0: Fundamental algorithms for scientific computing in Python. *Nature Methods*, 2020, 17: 261 – 272.